Progress on pulse shaping by compensating for temporal deformation in the Vulcan Nd:glass amplification chain

Contact: pedro.oliveira@stfc.ac.uk

J.A. Patel, L.E. Bradley, P. Oliveira, A. Kidd and I.O. Musgrave
Central Laser Facility
STFC Rutherford Appleton Laboratory
Harwell Campus
OXON. OX11 0QX

Abstract

The evolution of the temporal shape of a pulse as it passes through a Nd:glass amplifier chain is difficult to predict and depends on the gain and losses throughout the complete chain. We demonstrate that a time-dependent Frantz-Nodvik model can be employed to get a target output pulse shape. This allows us to calculate the ideal input pulse shape that will compensate for gain saturation from the Vulcan rod amplifier chain.

1 Introduction

In large-scale user facilities like the Vulcan laser [1], the problem of temporal pulse deformation is important to consider in order to deliver consistent pulse shapes. This occurs mainly due to time-varying transmission in optical gates (high voltage Pockels cells), and from gain saturation. In fact, in any laser amplifier, partial depletion of population inversion by the forefront of the pulse will reduce the gain for the rear of the pulse, and hence make the biggest contribution to temporal pulse deformation. Throughout the pulse, the gain will vary approximately as an exponential [2].

Deformation of the temporal profile becomes problematic in user experiments that require a precise envelope. This could be in inertial confinement fusion (ICF) [3] experiments, plasma physics high pressure experiments [4], or in warm dense matter experiments [5].

The Vulcan laser has been updated ever since its first inception in 1976 [6] and as a user facility in 2003 [1]. Thus far, the optics, amplifiers and flash lamps have often been replaced, and hence it is impractical to fully characterise every component. Prior to upgrades in Vulcan, the temporal pulse shape at the input was a flat-topped envelope, produced via a fast-shaping Pockels cell (PC). Recently, it has become possible to adapt the seed of the laser in the system, with the advent of temporally controllable pulse shapes [7]. However, in a single-shot system like Vulcan, it is not viable to use feedback loops or trial-and-error to obtain a target pulse shape at the end of the beamline, especially due to the 20 minute cooling time of the disk amplifiers [8], and shot-by-shot variations in the energy or alignment.

In this letter, we have used a time-dependent version of the Frantz-Nodvik equation [2, 9] to correlate the pulse shape between different points in the Vulcan long-pulse laser system. Vulcan is a multi-beam high-powered laser system, at the Central Laser Facility (RAL), which uses Nd:glass rod and disk amplifiers to reach up to the kilojoule energy level. In this model we consider only the Nd-doped phosphate (Schott LG-760) rod amplifier chain, shown in figure 1 (alongside the disk chain). The intention of this study is to be able to model and control the temporal deformations of the amplifiers for any future users that require more complex pulse shapes. We also aim at collecting the smallest amount of information to make this possible. The small-signal gain and the saturation fluence are the only details we require about each amplifier, together with the energy of the pulse through the chain.

2 Pulse shaping by modelling saturation

Consider an arbitrary normalised pulse given by $P(t) = I(t)/I_0$, with energy $\mathcal{E}$ and beam area A. The fluence is defined as

$$J = I_0 \int P(t)dt \tag{1}$$

where I_0 is the intensity peak of the input pulse

$$I_0 = \frac{\mathcal{E}}{A \int P(t)dt} \tag{2}$$

Our model uses a time-dependent version of the Frantz-Nodvik equation, which is derived from the rate equations [9], and predicts the amplified temporal output pulse $I_{out}(t)$ for a given input pulse $I_{in}(t)$:

$$I_{out}(t) = \frac{I_{in}(t)}{1 - (1 - G_0^{-1}) \exp(-J_{sat}^{-1} \int_{-\infty}^{t} dt' I_{in}(t'))} \tag{3}$$

where G_0 is the small-signal gain of the amplifier and J_{sat} is the saturation fluence of the gain medium. For photon energy $h\nu$, $J_{sat} = h\nu/(\sigma_{abs} + \sigma_{em})$, where σ_{abs} and σ_{em} are the respective absorption and emission cross-sections of the gain medium [10]. We obtain $J_{sat} = 4.20 \times 10^4$ Jm^{-2} at $\lambda = 1053$ nm, given that $\sigma_{abs} \sim 0$ for all Nd-doped gain media at $\lambda \sim 1$ μm, and that the amplifiers

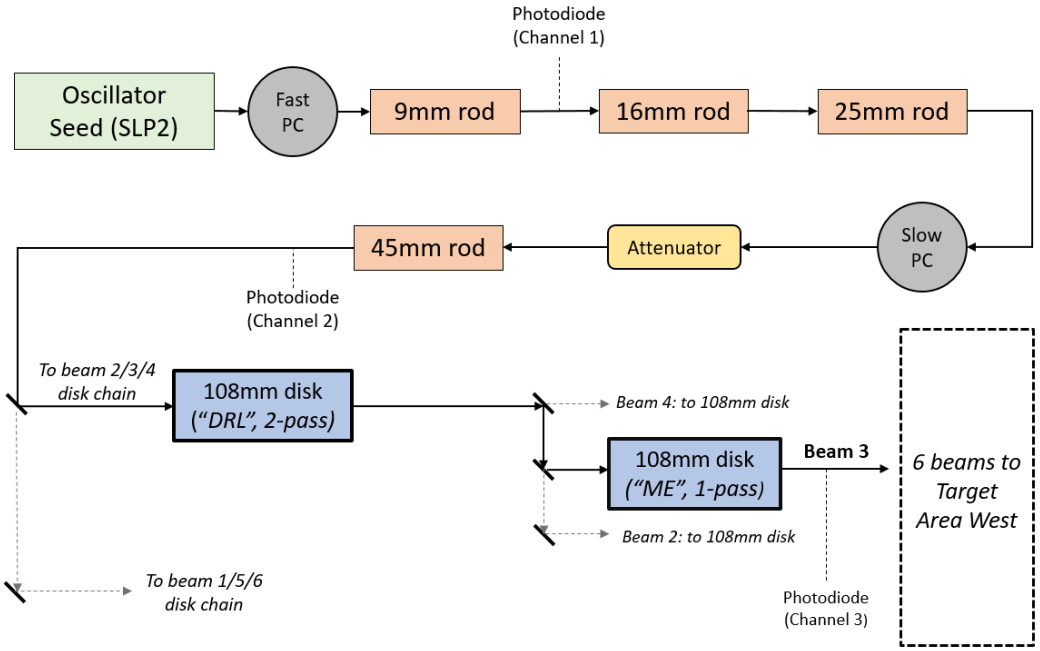

Figure 1: Simplified diagram of the Vulcan long-pulse rod and disk amplification chain. The three photodiodes are connected to the same Tektronix oscilloscope (DPO71254C).

have a known emission cross-section of $\sigma_{em} = 4.5 \times 10^{-24}$ m^2.

2.1 Validating the model by Miro simulations

We compared our analytical Frantz-Nodvik model, based entirely on eqn 3, with the MIRO optical propagation simulator. For each rod amplifier that was modelled, the small-signal gain was taken from table 1. For both models, we have plotted the predicted output pulse shape in figure 2 when a 1 ns ramp pulse is propagated through the rod amplifier chain. Our model appears to closely match the MIRO simulation.

Amplifier	Small-signal gain G_0 (estimate)
9 mm rod	20
16 mm rod	32
25 mm rod	12
45 mm rod	6
108 mm disk	10

Table 1: Estimations of the small-signal gain G_0 for each amplifier in the Vulcan long-pulse beamline, calculated using measurements of energy.

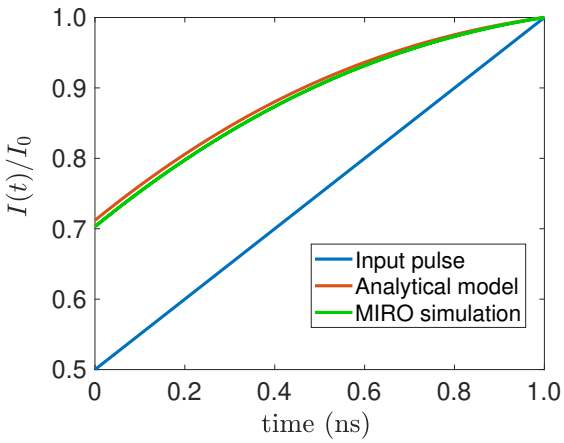

Figure 2: Simulated outputs in MIRO and our analytical model, when a 1 ns ramp pulse is propagated through the rod amplifier chain.

2.2 Observing saturation in the amplifier chain

We fired a 1 ns pulse into the system with all amplifiers switched on. In our system we have three photodiodes, shown in figure 1, respectively positioned after the 9 mm rod, after the 45 mm rod, and at the end of the disk chain. In figure 3 we present the behaviour of preferential gain at the start of the pulse as it propagated through the amplifier chain.

For each stage of amplification, the deformation is inherently dependent on the fluence J (and therefore the pulse energy). Our model currently relies on knowing the energies and losses at multiple points in the system, but this is impractical for our beamline. As such, in our model, we have made estimates on the losses.

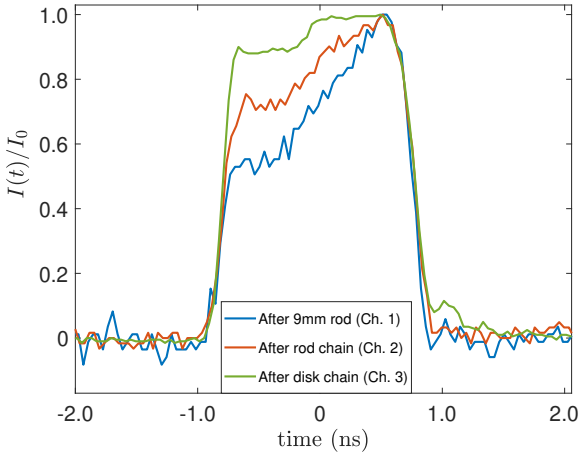

Figure 3: Observation of temporal deformation in the pulse at three stages of the amplifier chain (from figure 1).

2.3 *Verifying the saturation fluence and small-signal gain*

First, we checked the validity of the time-dependent Frantz-Nodvik model by confirming the saturation fluence J_{sat} of Nd:glass, using a least-squares minimisation algorithm. This method was employed to fit the saturated output shape $I_{out}(t)$ onto the arbitrary input $I_{in}(t)$. For this case, we have considered only the 45 mm amplifier for simplicity. The deformation from just the 45 mm amplifier was measured by comparing the traces from two separate test shots (with one having the 45 mm switched off). $I_{in}(t)$ is the trace with the 45 mm switched off, and $I_{out}(t)$ is the trace with it switched on (a normal test shot). Our algorithm is based on eqn 3, although now in terms of an optimal input pulse $I_{in}(t)$ for a given output pulse $I_{out}(t)$:

$$I_{in}(t) = \frac{I_{out}(t)}{1-(1-G_0)\exp(-J_{sat}^{-1}\int_0^t dt' I_{out}(t'))} \qquad (4)$$

Figure 5 shows the resulting fit $I_{fit}(t)$ from this minimisation algorithm. We obtained an experimental value of 4.33×10^4 Jm^{-2} which is in close agreement with the theoretical value (4.20×10^4 Jm^{-2}).

On the same set of data, we applied an algorithm that calculates the residual sum of squares d between $I_{out}(t)$ and $I_{in}(t)$ for different combinations of J_{sat} and small-signal gain G_0. For the 45 mm rod, $G_0 \sim 6$ (table 1) - this was calculated previously using measurements of energy. Figure 4 shows a colour-plot of d as a function of G_0 and J_{sat}. Taking $J_{sat} = 4.20 \times 10^4$ Jm^{-2}, we obtain $G_0 = 5.8$ for the 45 mm rod amplifier, which is consistent with theory.

The ideal case for the minimisation algorithm is when $I_{out}(t) > I_{in}(t)$ after the pulse is amplified. If however $I_{out}(t) \approx I_{in}(t)$ (negligible saturation), signal noise can cause the algorithm to fail and produce an unrealistic value. We are in the process of designing a Wiener filter that can be applied to our pulses. These are typically used in image and sound processing to remove noise via a deconvolution method [11]. Our intention is to be able to distinguish between noise and small amounts of saturation, and better reveal the temporal effects of other components in the system.

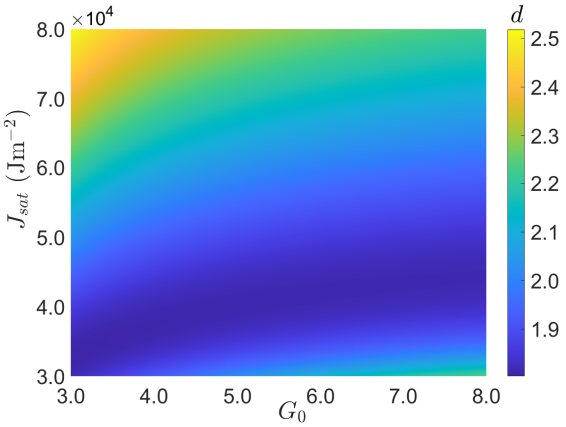

Figure 4: A colour-plot of the residual sum of squares d (between $I_{out}(t)$ and $I_{in}(t)$) as a function of saturation fluence J_{sat} and small-signal gain G_0.

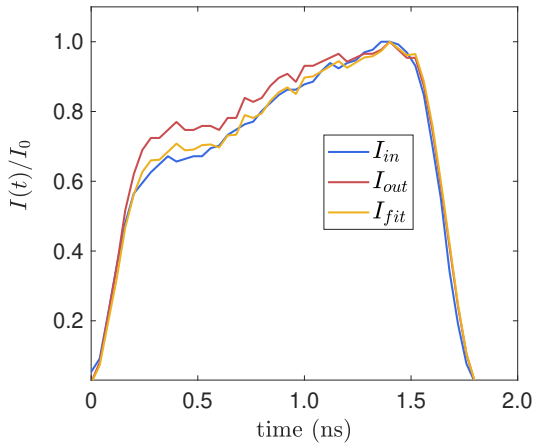

Figure 5: Photodiode waveforms for the input pulse shape $I_{in}(t)$, output pulse shape $I_{out}(t)$, and the fit $I_{fit}(t)$ after performing the minimisation algorithm.

3 Conclusion

In conclusion, we have shown that a simple model following the Frantz-Nodvik theory can be applied to the Vulcan amplifier chain. For our 45 mm rod amplifier, we have used this model to obtain an experimental value for the saturation fluence J_{sat} of Nd:glass (4.33×10^4

Jm^{-2}), which is consistent with the theoretical value of 4.20×10^4 Jm^{-2}. Our model also matches the MIRO propagation simulator.

In the future, we plan on developing this model so that it simulates the deformation from the DRL (double-pass) and ME (single-pass) 108 mm disk amplifiers.

References

[1] I. Musgrave, G. Archipovaite, S. Blake, N. Booth, O. Chekhlov, R. Clarke, R. Heathcote, C. Hernandez-Gomez, M. Galimberti, M. Galletti, P. Oliveira, D. Neely, W. Shaikh, T. Winstone, J. Collier, and B. Wyborn, "Development of a PW class OPCPA beamline for the Vulcan Laser Facility (Conference Presentation)," in *Short-pulse High-energy Lasers and Ultrafast Optical Technologies* (P. Bakule and C. L. Haefner, eds.), vol. 11034, International Society for Optics and Photonics, SPIE, 2019.

[2] L. M. Frantz and L. S. Nodvik, "Theory of pulse propagation in a laser amplifier," *J. Appl. Phys.*, vol. 34, no. 2346-2349, 1963.

[3] H. F. Robey *et al.*, "The effect of laser pulse shape variations on the adiabat of NIF capsule implosions," *J. Appl. Phys.*, vol. 20, no. 5 052707, 2013.

[4] H. Nagao, K. G. Nakamura, K. Kondo, N. Ozaki, K. Takamatsu, T. Ono, T. Shiota, D. Ichinose, K. A. Tanaka, K. Wakabayashi, K. Okada, M. Yoshida, M. Nakai, K. Nagai, K. Shigemori, T. Sakaiya, and K. Otani, "Hugoniot measurement of diamond under laser shock compression up to 2TPa," *Physics of Plasmas*, vol. 13, no. 5, p. 052705, 2006.

[5] R. Torchio, F. Occelli, O. Mathon, A. Sollier, E. Lescoute, L. Videau, T. Vinci, A. Benuzzi-Mounaix, J. Headspith, W. Helsby, S. Bland, D. Eakins, D. Chapman, S. Pascarelli, and P. Loubeyre, "Probing local and electronic structure in warm dense matter: single pulse synchrotron x-ray absorption spectroscopy on shocked Fe," *Scientific Reports*, vol. 6, pp. 26402 EP –, Jun 2016. Article.

[6] H. F. Robey *et al.*, "Annual report to the laser facility committee," vol. RL-78-039, 1978.

[7] P. Oliveira, S. Addis, J. Gay, K. Ertel, M. Galimberti, and I. Musgrave, "Control of temporal shape of nanosecond long lasers using feedback loops," *Opt. Express*, vol. 27, pp. 6607–6617, Mar 2019.

[8] M. M. J Boon, C Danson, "Diameter 108 disc amplifier amplifier cooling," vol. RAL-85-047, A6.3.3.

[9] D. N. Schimpf and others., "Compensation of pulse-distortion in saturated laser amplifiers," *Opt Exp*, vol. 16, no. 22, 2008.

[10] R. Paschotta, "RP Photonics - Four-level and Three-level Gain Media." `https://www.rp-photonics.com/four_level_and_three_level_gain_media.html`, Oct 2019.

[11] R. C. Gonzalez and R. E. Woods, *Digital Image Processing*. Prentice Hall, 2008.